Richard Volpe

Jet Propulsion Laboratory
California Institute of Technology
Pasadena, California 91109

Pradeep Khosla

Department of Electrical and Computer Engineering
The Robotics Institute
Carnegie Mellon University
Pittsburgh, Pennsylvania, 15213

The Equivalence of Second-Order Impedance Control and Proportional Gain Explicit Force Control

Abstract

This article discusses the essential equivalence of second-order impedance control with force feedback and proportional gain explicit force control with force feedforward. This is first done analytically by reviewing each control method and showing how they mathematically correspond for constrained manipulator control. For stiff environments the correspondence is exact. However, even for softer environments, a similar response of the system is indicated. Next, the results of an implementation of these control schemes on the CMU DD Arm II are presented, confirming the predictions of the analysis. These results experimentally demonstrate that proportional gain force control and impedance control, with and without dynamics compensation, have equivalent response to commanded force trajectories.

1. Introduction

There is an entire class of tasks that implicitly require controlling the force of interaction between a manipulator and its environment: pushing, scraping, grinding, pounding, polishing, twisting, etc. Thus, force control of the manipulator becomes necessary in at least one of the degrees of freedom of the manipulator; the other degrees of freedom remain position controlled. Mason (1981) formalized this idea and called it *hybrid control*. Simply put, the manipulator should be force controlled in directions in which the position is constrained by environmental interaction, and position controlled in all orthogonal directions.

The hybrid control formalism does not specify what particular type of position or force control should be used. It only partitions the space spanned by the total degrees of freedom into one subspace in which position control is employed, and another in which force control is employed. In the position control subspace, simple strategies have proven adequate (e.g., PID), while sophisticated enhancements have improved performance (e.g., computed torque control, adaptive control) (Dubowsky and DesForges 1979; Koivo and Guo 1981; Hsia 1986; Slotine and Li 1987; Khosla 1988). However, in the force control subspace, two main conceptual choices have emerged: *explicit force control* and *impedance control*. Figure 1 shows two simple block diagrams of these control schemes; the transfer function G represents the dynamics of the arm/sensor/environment system, H is the force controller, I is the impedance controller, and u is the control signal. The major difference between these schemes is the commanded value: explicit force control requires commanded force, while impedance control requires commanded position. In order for these to be feedback controllers, explicit force control needs force measurement, while impedance control needs position measurement. In addition, impedance control requires force measurement; without it an impedance controller reduces to a position controller.

Ideally, an explicit force controller attempts to make the manipulator act as a pure force source, independent of position. Like position control, the obvious first choice has been some manifestation of PID control (i.e., P, PD, PI, etc.). We have previously shown that integral gain control is the best among these simple strategies (Volpe and Khosla 1993a).

Alternatively, impedance control has been presented as a method of stably interacting with the environment. This is achieved by providing a dynamic relationship between the robot's position and the force it exerts. A complete introduction to impedance control is beyond the scope of this discussion, and the reader is referred to the previous work of other researchers (Hogan 1985; Kaze-

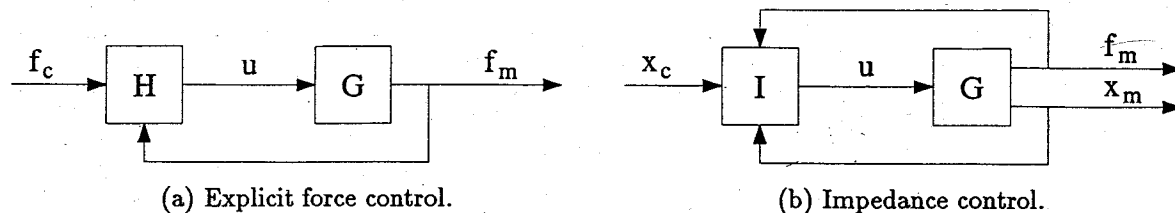(a) Explicit force control.   (b) Impedance control.

Fig. 1. Block diagrams of the two main types of force regulation.

rooni et al. 1986). The basic tenet of impedance control is that the arm should be controlled so that it behaves as a mechanical impedance to positional constraints imposed by the environment.

For linear impedance relationships, the controller may be separated into two transfer functions, $I(x)$ and $I(f)$. With these functions, the impedance control block diagram is modified as in Figure 2 to show that the impedance controller contains an internal explicit force controller. Furthermore, the feedback term, x_m, may be ignored sometimes. For instance, it may be ignored if its variation is slow compared to the dynamics of the close loop system or if the magnitude change is smaller than the resolution of the position measuring capabilities of the system. In these cases, the system may be considered open loop with respect to position and velocity, and impedance control reduces directly to explicit force control.

This article explores the exact correspondence between explicit force control and impedance control. In particular, it is shown that impedance controllers that utilize force feedback must be second order; lesser order impedance relations are essentially open-loop to force (Volpe and Khosla 1991; Goldenberg 1992). Analysis of the second-order impedance controller reveals that it has an algebraic structure akin to proportional gain explicit force control with feedforward reference force. This correspondence becomes exact when the position feedback is constant. In practice, this criterion is regularly met by stiff environments or soft environments in equilibrium with the arm.

We have implemented both impedance control with and without manipulator dynamics compensation, as well as proportional gain explicit force control. These implementations were in six DOFs on the CMU DD Arm II. The results show the same response for the impedance and explicit force control strategies, even for the case of soft environment contact. They also experimentally confirm what is analytically indicated: the equivalence of second-order impedance control with force feedback and proportional gain force control with reference force feedforward.

This article is organized as follows. First, the arm and environment models employed for this discussion will

be reviewed. Second, proportional gain explicit force control is reviewed and analyzed. It is also shown how the proportional gain values can be as low as negative one. Third, impedance control, with and without dynamics compensation, is reviewed and analyzed. It is shown that only second-order impedance control utilizes force feedback information. It is also shown that second-order impedance control employs proportional gain explicit force control, and that for stiff environments the two become the same controller. In the last part of this article, the insights and predictions from analysis of the controllers are experimentally verified with force-trajectory and impact tests.

2. Arm/Sensor/Environment Model

The physical system employed in this study comprises the CMU DD Arm II, a Lord 15-50 force sensor, and an environment of a cardboard box with an aluminum plate resting on top. The box rests on a table that is considerably more stiff than the box and is therefore considered ground for these tests. The force sensor is mounted on link 6 of the CMU DD Arm II. Attached to the force sensor is a steel probe with a brass weight on its end. The brass weight serves as an end-effector substitute and provides a flat, stiff surface for applying forces on the environment. More details can be found in Volpe and Khosla 1993b; 1994a).

This system is more complex than might first be thought. Since the arm is not attached to the surface, oscillations can easily lead to separation from the surface. In the case of separation, the system plant is *nonlinear*. Furthermore, we have previously discussed how attachment to the environment (as with a gripper) increases the envelope of stability (Volpe and Khosla 1993). For the discussion and experiments presented in this article, the system will be modeled without separation, but no physical attachment is made.

Previous research has indicated that a fourth-order model of the arm/sensor/environment as shown in Figure 3, is necessary for force control analysis (Eppinger and Seering 1986; Volpe and Khosla 1994a). The transfer
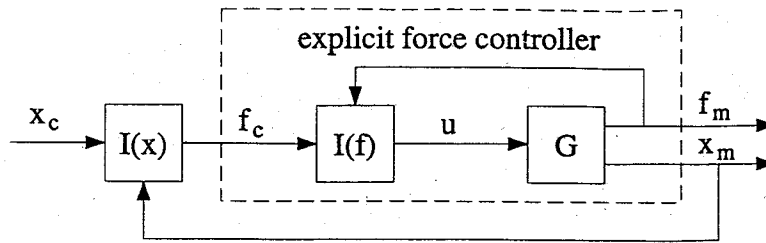
Fig. 2. Impedance control block diagram redrawn to show the inner explicit force controller.

function of this system is:

$$G = \frac{F_m}{U} = \qquad (1)$$

$$\frac{(m_B s^2 + c_3 s + k_3)k_2}{\begin{array}{c}(m_B s^2 + (c_2 + c_3)s + (k_2 + k_3)) \\ (m_A s^2 + c_1 s + k_1) + (m_B s^2 + c_3 s + k_3)(c_2 s + k_2)\end{array}}$$

where the measured force, F_m, is equal to $k_2(x_A - x_B)$. We have experimentally extracted parameter values for the components of this model for the box/plate environment described. Mathematical and experimental details can be found elsewhere (Volpe and Khosla 1994a).

The pole/zero locations indicated by the extracted parameters differ greatly from those assumed by other researchers (Eppinger and Seering 1986; 1987). Figure 4 shows all but the leftmost pole, which is at $-28,000$ on the real axis. The complex pole pair (with real value ≈ -12) is due mainly to the environment. The other pole pair (on the real axis) is due mainly to the sensor dynamics. It can be seen that the sensor poles are fairly far removed from the environmental ones, and are located farther into the left half-plane. The leftmost sensor pole (at $-28,000$) will be ignored.

Utilizing the plant model developed, it is now possible to analyze its response with both proportional gain explicit force control and impedance control. This will be done in the following sections.

3. Proportional Gain Explicit Force Control

The first controller to be discussed is proportional gain explicit force control. The chosen form of this controller is:

$$\tau = \mathbf{J}^T \mathbf{u} + \mathbf{g}, \qquad (2)$$

where τ is a vector of the actuation torques, $\mathbf{J}$ is the manipulator Jacobian, $\mathbf{g}$ is the gravity compensation torque vector, and $\mathbf{u}$ is the control signal vector comprising components (Volpe and Khosla 1993a):

$$u = f_c + K_{fp}(f_c - f_m) - K_v \dot{x}_m, \qquad (3)$$

where subscripts c and m denote the commanded and measured quantities, respectively. The feedforward term,

f_c, is necessary to provide a bias force when the force error is zero. Since the velocity gain, K_v, adds damping directly to the system plant, G, the closed-loop transfer function with the feedforward term is:

$$\frac{F_m}{F_c} = \frac{(1 + K_{fp})G}{1 + K_{fp}G}. \qquad (4)$$

This is a Type 0 System and will have a nonzero steady-state error for a step input. The root locus of this system is shown in Figures 4 and 5. The corresponding Bode plots are shown in Figure 6. As can be seen from the root locus, proportional control makes the system more oscillatory and can make it unstable. The Bode plots further illustrate this problem. There is a resonance peak from the environment dynamics at approximately $100\,\text{rad/s}$. After this peak there is a 40-dB/decade drop-off, which gives a minimum phase margin of $\sim 15°$ at $K_{fp} \approx 1$.

The addition of a low-pass filter in the feedback loop can improve the response by introducing a dominant pole on the real axis (An and Hollerbach 1987). However, this pole placement and the resultant behavior of the system closely match that provided by integral control (Volpe and Khosla 1993a), and therefore it will not be considered further.

It will prove useful later (in the discussion of impedance control) to review the consequences of using the feedforward term in equation (3) (Volpe and Khosla 1993b). It is usually desirable that the feedforward gain be unity so that the environmental reaction force will be canceled during steady state. Furthermore, if the sensor dynamics of the plant are ignored and the natural feedback loop of the reaction force is considered, the plant may be reformulated as $G = G'/(1 + G')$, where G' represents the dynamics of the arm/environment only. Substitution of this reduced model into the transfer function of equation (4) yields:

$$\frac{F_m}{F_c} = \frac{(1 + K_{fp})G'}{1 + (1 + K_{fp})G'} \qquad (5)$$

$$= \frac{K'_{fp}G'}{1 + K'_{fp}G'}, \qquad (6)$$

where $K'_{fp} = 1 + K_{fp}$. Thus, the proportional gain of the original controller, K_{fp}, may be as small as negative one.
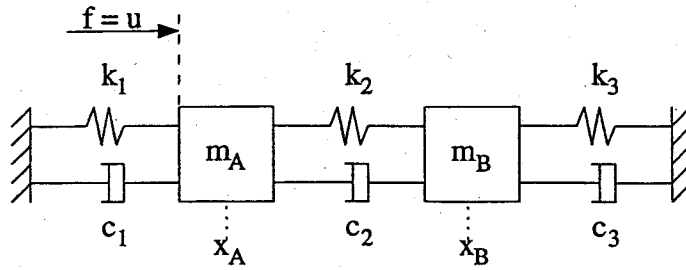
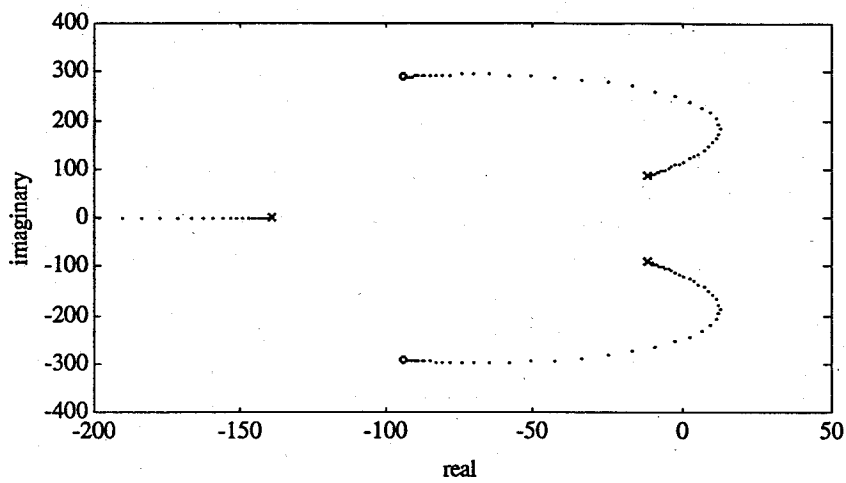Fig. 3. General fourth-order model of the arm, sensor, and environment system.

Fig. 4. Root locus for the fourth-order model under proportional gain explicit force control ($K_{fp} \geq 0$).
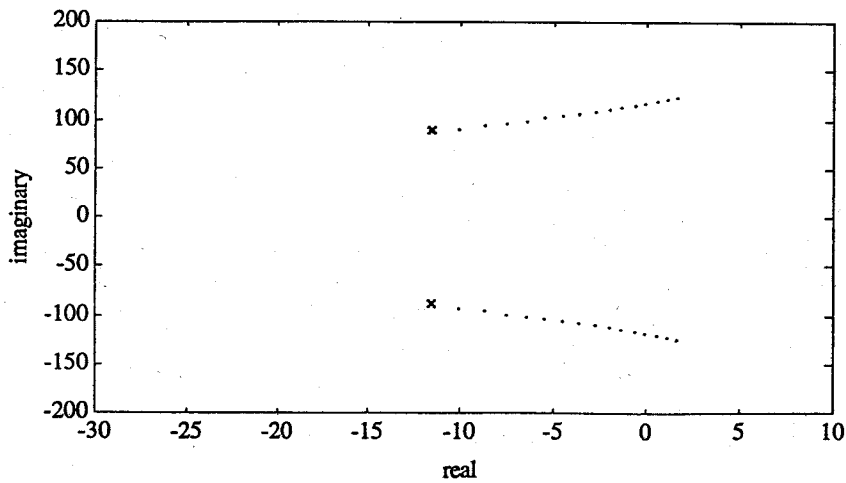

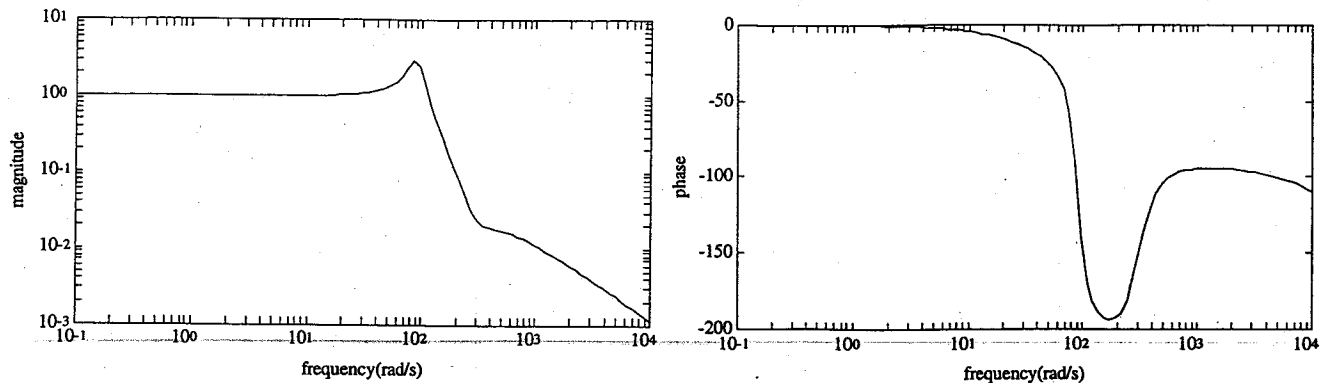Fig. 5. Enlargement of the root locus in figure 4 with K_{fp} values of 0 to 1.5 in steps of 0.1.

Fig. 6. Bode plots for the fourth-order system under proportional gain explicit force control. The resonance peak occurs near the natural frequency of the environment. The gain margin is 1.2 at $\omega = 118\,rad/s$, which corresponds to the root locus crossing to the right half-plane in Figure 5.

Figure 7 shows the proportional gain force control root locus for gains as low as -1. We have previously shown the utility of negative gains for impact control (Volpe and Khosla 1993b). Other researchers have also discussed the use of negative gains, but usually within the context of impedance control (Hamilton 1988; Hogan 1987). It will be seen in the following sections that the impedance controllers for which this result was obtained actually contain proportional gain explicit force control.

4. Second-Order Impedance Control

Impedance control is a strategy that controls the dynamic relation between the manipulator and the environment. The force exerted on the environment by the manipulator is dependent on its position and its impedance. Usually this relation is expressed in Cartesian space as:

$$f = \mathcal{Z}(x), \tag{7}$$

where f, x, and $\mathcal{Z}$, are force, position, and impedance. The impedance consists of two components: that which is physically intrinsic to the manipulator, and that which is given to the manipulator by active control. It is the goal of impedance control to mask the intrinsic properties of the arm and replace them with the target impedance.

The impedance relation can have any functional form. It has been shown that general impedances are useful for obstacle avoidance (Hogan 1985; Khatib 1986; Volpe and Khosla 1990). However, it will be made clear in this section that sensor-based, feedback-controlled interaction with the environment is best achieved if the impedance is linear and of second order at most. This is for two reasons. First, the dynamics of a second-order system

are well understood and familiar. Second, for higher order systems, it is difficult to obtain measurements for closed-loop control corresponding to the higher order state variables.

To implement impedance control, model-based control can be used. This type of scheme relies on the inverse of the Jacobian. A second type of controller that uses the transpose of the Jacobian is sometimes employed. Both forms of impedance control will be shown to contain proportional gain explicit force control (with feedforward force). Also, if the position feedback is essentially constant, as when in contact with an environment of any appreciable stiffness, impedance control reduces directly to proportional gain force control.

The next sections are organized as follows. First, the order of the desired impedance will be discussed, and the implications for implementation will be shown. Second, model-based impedance control will be reviewed, and the reduced form of impedance control without dynamics compensation will presented. Third, it will be shown how each of these schemes contains an internal proportional gain force control loop that will determine the system response when in contact with a stiff environment.

4.1. Zeroth, First-, and Second-Order Impedance

A linear impedance relation may be represented in the Laplace domain as:

$$F = Z(s)X. \tag{8}$$

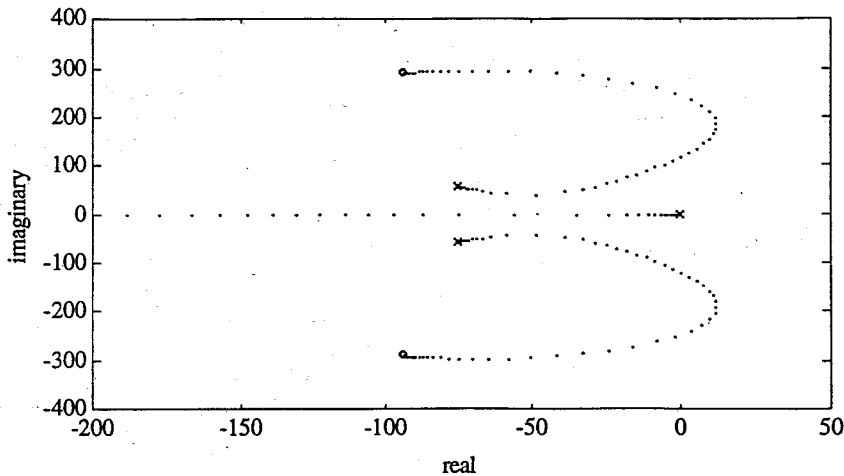The order of the polynomial $Z(s)$ is considered the order of the impedance.

Fig. 7. Root locus for the fourth-order model for $-1 \leq K_{fp} < \infty$ or $0 \leq K'_{fp} < \infty$.

The simplest form of an impedance controller has a zeroth order impedance. In this case Z is a constant and

$$F = KX. \qquad (9)$$

The impedance parameter K is the desired stiffness of the manipulator and is typically determined by the sum of the actuator and controller stiffnesses. If the actuators have no intrinsic stiffness (as in the case of the CMU DD Arm II), the active position feedback gain dictates the apparent stiffness of the arm.

A more typical form of an impedance controller is a first-order impedance. In this case,

$$F = (Cs + K)X. \qquad (10)$$

The added parameter C is the desired damping of the manipulator and is equal to the sum of the active and natural damping. Since active damping can be modified, C can take on any value that maintains stability. In fact, negative active damping can be used to eliminate the appearance of any damping in the arm (due to gear friction and other causes). This is rarely desirable, since damping has a stabilizing effect.

Finally, a more complete form of impedance control is provided by the second-order type,

$$F = \left(Ms^2 + Cs + K\right)X. \qquad (11)$$

The parameter M is the desired inertia of the manipulator. While the intrinsic inertia of the arm is due to its mass, it can be modified by active feedback. From the previous two cases, it follows that acceleration feedback can be used for this purpose. In this case, the value of active inertia is the acceleration feedback gain, and its value can be used to adjust M. Few researchers have proposed such acceleration feedback schemes for impedance control (Goldenberg 1988; Tourassis 1988). This is because

an acceleration measurement typically requires a second derivative, which will be extremely noisy. Alternatively, the force may be measured and the acceleration commanded. This is typically the method employed, as will be shown.

4.2. Manipulator Model–Based Control

Manipulator model–based control involves the use of a dynamic model of the manipulator to determine the actuation torques, τ (Bejczy 1974). Model–based impedance control may be summarized by the following equations (Hogan 1985; Volpe 1990):

$$\tau = \mathbf{D}(\theta_m)\mathbf{u} + \mathbf{h}(\theta_m, \dot{\theta}_m) + \mathbf{g}(\theta_m) + \mathbf{J}^T(\theta_m)\mathbf{f}_m \qquad (12)$$

$$\mathbf{u} = \mathbf{J}^{-1}(\theta_m)\left[\ddot{\mathbf{x}}_u - \dot{\mathbf{J}}(\theta_m)\dot{\theta}_m\right] \qquad (13)$$

$$\ddot{\mathbf{x}}_u = \mathbf{M}^{-1}\left[\mathbf{C}\Delta\dot{\mathbf{x}} + \mathbf{K}\Delta\mathbf{x} - \mathbf{f}_m\right] \qquad (14)$$

$$\Delta\mathbf{x} = \mathbf{x}_c - \mathcal{F}(\theta_m) \qquad (15)$$

$$\Delta\dot{\mathbf{x}} = \dot{\mathbf{x}}_c - \mathbf{J}(\theta_m)\dot{\theta}_m. \qquad (16)$$

Equation (12) compensates for the dynamics of the manipulator with inertia matrix $\mathbf{D}$, Coriolis and centripetal force vector $\mathbf{h}$, and gravitational force vector $\mathbf{g}$. Equation (13) describes the control signal in terms of the desired Cartesian acceleration. Equation (14) specifies the desired second-order impedance control relationship. Matrices $\mathbf{M}$, $\mathbf{C}$, and $\mathbf{K}$ describe the desired impedance and are typically specified with scalar values M, C, and K along the diagonal. Equations (15) and (16) determine the Cartesian position and velocity errors through the forward kinematics, $\mathcal{F}(\theta_m)$, and the manipulator Jacobian, $\mathbf{J}(\theta_m)$. The subscripts c and m indicate commanded and measured quantities of the joint and Cartesian position vectors, θ and $\mathbf{x}$.

Without force feedback this control scheme is equivalent to position control schemes such as Resolved Acceleration Control (Luh et al. 1980) and Operational Space Control (Khatib 1980). These are first-order impedance control schemes, since they only modify the stiffness and damping of the arm. Including force feedback information in the controller yields second-order impedance control (Hogan 1985). Combining the above equations gives:

$$\tau = \mathbf{DJ}^{-1}\mathbf{M}^{-1}(\mathbf{C}\Delta\dot{\mathbf{x}} + \mathbf{K}\Delta\mathbf{x} - \mathbf{f}_m)$$
$$- \mathbf{J}^{-1}\dot{\mathbf{J}}\dot{\theta} + \mathbf{h} + \mathbf{g} + \mathbf{J}^T\mathbf{f}_m \quad (17)$$

or

$$\tau = \mathbf{J}^T\Lambda\mathbf{M}^{-1}(\mathbf{C}\Delta\dot{\mathbf{x}} + \mathbf{K}\Delta\mathbf{x} - \mathbf{f}_m)$$
$$- \mathbf{J}^T\Lambda\dot{\mathbf{J}}\dot{\theta} + \mathbf{h} + \mathbf{g} + \mathbf{J}^T\mathbf{f}_m \quad (18)$$

where

$$\mathbf{D}(\theta) = \mathbf{J}^T\Lambda(\mathbf{x})\mathbf{J} \quad (19)$$

and the matrix, Λ, is the Cartesian space representation of the inertia matrix. The first form is necessary if the inverse dynamics calculations expressed in equation (12) are used. In this case, the inverse of the Jacobian and the arm inertia must be calculated. The second form is useful when employing the steady-state approximation in which the manipulator inertia is assumed not to change or is not known (Kazerooni et al. 1986). In this case, $\dot{\mathbf{J}}$ as well as $\mathbf{h}$ will equal zero also:

$$\tau = \mathbf{J}^T\Lambda\mathbf{M}^{-1}(\mathbf{C}\Delta\dot{\mathbf{x}} + \mathbf{K}\Delta\mathbf{x} - \mathbf{f}_m) + \mathbf{g} + \mathbf{J}^T\mathbf{f}_m. \quad (20)$$

For the case of steady state, the inverse of the Jacobian need not be calculated; only its transpose is necessary. The arm inertia need not be calculated either, since only its product with the inverse of the impedance mass parameter is needed, as will be explained shortly.

Note that in manipulator model–based control, the force feedback is used in two places. First, it is used to compensate for the physical arm dynamics through equation (12). This is equivalent to introducing end-effector forces into the inverse dynamics calculations. Second, the force feedback is used in the impedance relation, equation (14). While equation (12) effectively linearizes the dynamics of the arm, equation (14) modifies the impedance control signal to compensate for the experienced force.

It can now be seen that it is the force feedback in the control signal that modifies the apparent inertia of the arm (Hogan 1987). Equation (20) best shows this effect. The premultiplication of $\mathbf{K}$ and $\mathbf{C}$ by $\Lambda\mathbf{M}^{-1}$ changes nothing; $\Delta\dot{\mathbf{x}}$ and $\Delta\mathbf{x}$ are still multiplied by a gain. However, things are made different by the force feedback signal $\mathbf{f}_m$. It is multiplied by the term $\Lambda\mathbf{M}^{-1}$, which is a mass ratio that reduces or increases the amount of actuator torque applied.

The description may be simplified by assuming that the impedance matrices are diagonal in the Cartesian space defined by the eigenvectors of Λ. In this case, $\Lambda\mathbf{M}^{-1}$ can be thought of as a matrix of mass ratios, Λ/M, along the diagonal. Since Λ is due to the physical inertia of the arm, it is the impedance parameter M that determines each ratio. For $M \to 0$, the ratio becomes very large; for a small measured force, a large accelerating torque is applied to the arm. Thus, the apparent inertia of the arm is reduced. (It is important to remember that the external force does not contribute to the acceleration, because it has been effectively negated by the $\mathbf{J}^T\mathbf{f}_m$ term.) Similarly, for $M' \to \infty$, the ratio becomes very small; for a large measured force, a small accelerating torque is applied to the arm. Thus, the apparent inertia of the arm is increased. In this way, second-order impedance control changes not only the stiffness and damping properties of the arm, but its inertia as well.

4.3. Explicit Force Control Within Impedance Control

The two second-order impedance controllers reviewed above can be shown to contain explicit force control. Previous to our research, some correspondence between impedance control and explicit force control has been discussed, but the relation was not specifically or clearly stated (Hogan 1987; Anderson and Spong 1988). A general argument supporting our new interpretation was presented in the introduction and elsewhere (Volpe and Khosla 1993b). Now it will be shown explicitly for the impedance controllers described previously in this article.

Consider the second-order impedance controller represented by equation (20). This can be rewritten in the form:

$$\tau = \mathbf{J}^T\left[\mathbf{f}_c + \mathbf{K}_{fp}(\mathbf{f}_c - \mathbf{f}_m) - \mathbf{K}_v\dot{\mathbf{x}}_m\right] + \mathbf{g} \quad (21)$$
$$\mathbf{f}_c = \mathbf{K}(\mathbf{x}_c - \mathbf{x}_m) + \mathbf{C}\dot{\mathbf{x}}_c \quad (22)$$
$$\mathbf{K}_{fp} = \Lambda\mathbf{M}^{-1} - 1 \quad (23)$$
$$\mathbf{K}_v = \Lambda\mathbf{M}^{-1}\mathbf{C} \quad (24)$$

Again, the impedance parameters, $\mathbf{K}$ and $\mathbf{C}$, may be specified in the frame in which Λ is diagonal. This makes the gains diagonal and composed of the elements, K, C, and

$$K_{fp} = (\Lambda/M) - 1 \quad (25)$$
$$K_v = (\Lambda/M)C \quad (26)$$

This formulation is very similar to the proportional gain explicit force controller in equations (2) and (3). The only difference is the presence of equation (22). However, when in contact with an environment of appreciable stiffness, this equation reduces directly to commanding force. First, the measured position, $\mathbf{x}_m$, will be constant

and can be set to zero. Typically this is because the surface motion is smaller than the measurement resolution of the manipulator (Volpe and Khosla 1994b). Second, most contact occurs with surfaces that are stationary during equilibrium, indicating that the commanded velocity should be zero ($\dot{\mathbf{x}}_c = 0$). This leaves only $\mathbf{x}_c$ as nonzero. It provides the commanded force by direct multiplication with the stiffness, $\mathbf{K}$. This means that the commanded position is scaled to provide commanded force, which could more simply be provided directly. Therefore, equation (22) may be eliminated, and the impedance controller reduces directly to proportional gain force control. Since all of the gains are diagonal and independently adjustable, this controller has an identical structure to the explicit force controller in equation (3).

In the case of softer environments, the compression of the surface by $\delta\mathbf{x}_m$ will cause only a small change, $\delta\mathbf{f}_c$, in the commanded force. The relative change is proportional to the ratio of the arm stiffness to the environment stiffness:

$$\frac{|\delta\mathbf{f}_c|}{|\mathbf{f}_c|} = \frac{|\delta\mathbf{x}_m|}{|\mathbf{x}_c - \delta\mathbf{x}_m|} = \frac{K}{K_{env}}. \tag{27}$$

Therefore, environmental stiffness at least an order of magnitude greater than the arm stiffness will essentially result in continued equivalence of the control schemes. With environments that are known to be even softer, if the commanded position is modified to compensate for the surface compression, the schemes continue to be equivalent. In the extreme case of an environment with no appreciable stiffness, the equivalence breaks down completely. However, force control is probably not meaningful in this unconstrained situation.

Finally, the developed formulation not only shows the equivalence of the two schemes, it also shows how the target impedance mass relates to the proportional force gain. Previously, the force gain was shown to be $K_{fp} = (\Lambda/M) - 1$, with a lower stability bound of $K_{fp} \geq -1$ or

$$\Lambda/M \geq 0. \tag{28}$$

This implies that the open loop pole location of the root locus corresponds to the impedance parameter $M \to \infty$, and the zeros indicate a value of $M \to 0$. This also means that large impedance target mass is the same as small proportional force gain, and small mass is the same as large gain.

5. Experimental Results

This section presents the experimental results of implementations of proportional gain force control with feedforward and second-order impedance control with and without dynamics compensation. It will be seen that in each case, the response and stability of the system are essentially the same.

The experiments presented here were conducted with the manipulator pressing down on an environment composed of a cardboard box with an aluminum plate resting on top, as described in Section 2. The parameters of a second-order model of this environmental system were: stiffness, $k \approx 10^4$ N/m; damping, $c \approx 17$ N·s/m; and mass, $m \approx 0.1$ kg (Volpe and Khosla 1994a).

All experiments were conducted using the CMU DD Arm II. This manipulator has very straightforward dynamics, making the analysis and interpretation of experimental results easier. Furthermore, the direct drive arm has essentially frictionless joints, eliminating the possibility of intrinsic damping, which can add stability to the system and hide problems inherent in the controller. Controllers that perform stably with the DD Arm will most likely remain stable on heavily geared and damped systems, whereas the converse is not true.

The controllers were programed in the C language, under the Chimera real-time operating system (Stewart et al. 1992). The control rate was 300 Hz, except in the case of dynamics compensation, where it was 250 Hz. All graphs of data show the reference values as a dashed line and the measured values as a solid line.
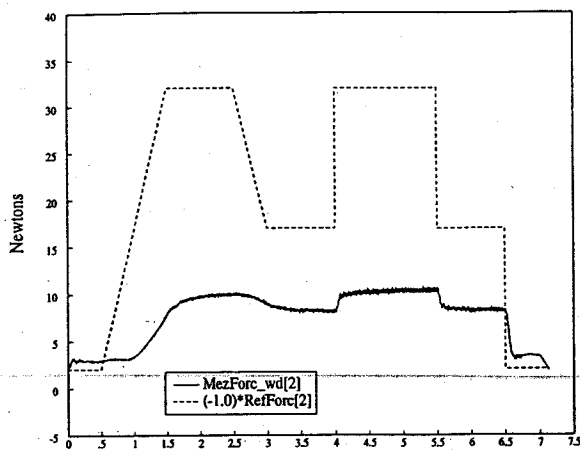
5.1. Proportional Gain With Feedforward Control

The first controller to be discussed is proportional gain force control with the reference force feedforward, equations (2) and (3). Figure 8 shows the response of this controller to the commanded force trajectory. In all experiments the velocity gain was $K_v = 10$. There are several things to note about the response profiles to variations in the proportional gain. First, as predicted by the model, the system exhibits the characteristics of a Type 0 system: finite steady-state error for a step input and unbounded error for a ramp input. Second, for an increase in position gain, the steady-state error reduces, but at the cost of increasingly larger overshoot. As correctly predicted by the root locus of the system model in Figure 5, this control scheme causes instability at $K_{fp} \approx 1$. Also, the fact that the environmental poles are always off the real axis can be seen in the steady-state oscillations that occur at the system's natural frequency (~ 15 Hz), particularly after the step input. Finally, it can be seen that negative proportional gains are increasingly more stable, but the response of the system approaches zero as $K_{fp} \to -1$.

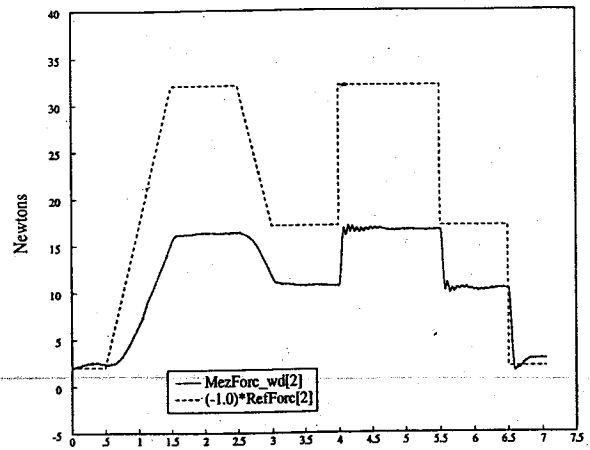## 5.2. Impedance Control

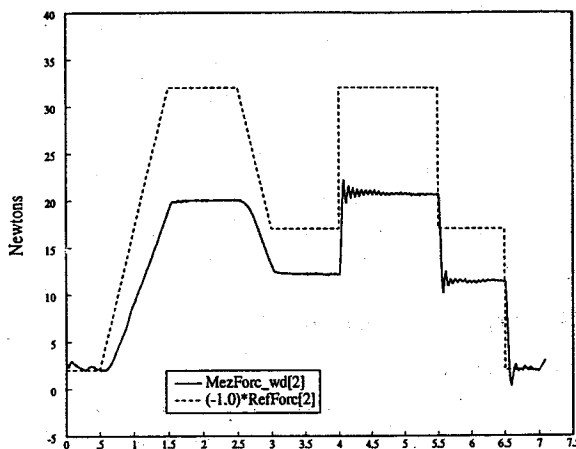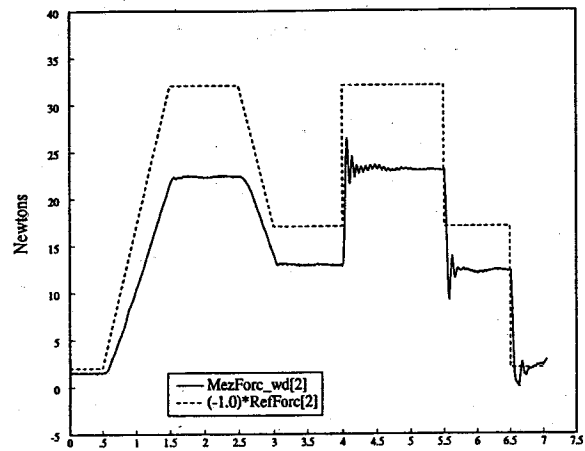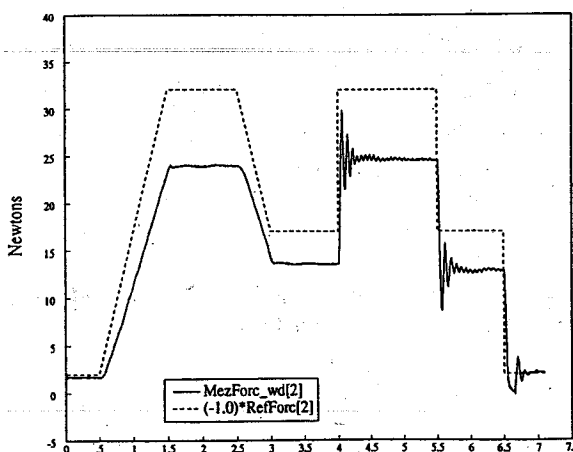This section presents the results of implementing second-order impedance control, with and without dynamics

Fig. 8. Experimental data of proportional gain explicit force control with feedforward. The proportional gain varies from −0.75 to 1.

(g) $K_{fp} = 0.75$ Time(seconds) **(h)** $K_{fp} = 1$ Time(seconds)
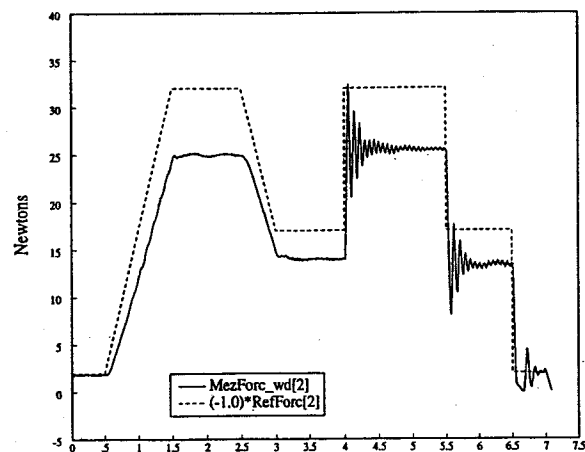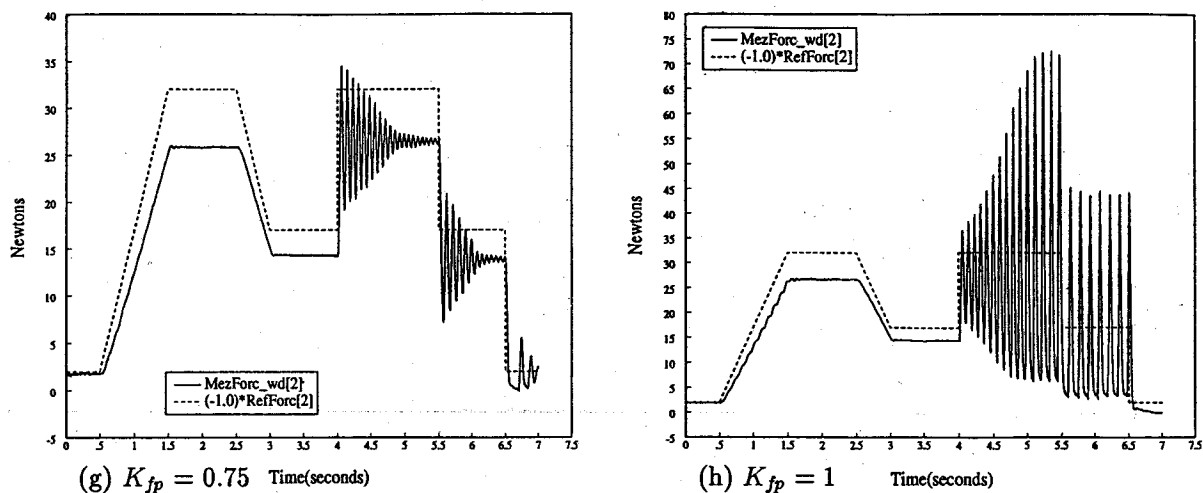
Fig. 8. continued. Experimental data of proportional gain explicit force control with feedforward. The proportional gain varies from −0.75 to 1.

compensation. The position reference trajectories are chosen such that, given the stiffness of the controller, the trajectory should provide the same force profile as commanded for the proportional gain explicit force controller, allowing a direct comparison with that controller.

5.2.1. Impedance Control Without Dynamics Compensation

When in contact with a stiff environment, the manipulator will not move very much or very quickly in the direction normal to the environment. It was shown previously that this enables a steady-state approximation, eliminating the need to calculate the inverse dynamics and the inverse Jacobian. The control law has the form of equation (20). For these experiments $K = 150\,\mathrm{N/m}$ and $C = 10$ N/m·s. As discussed in Section 4.3, the mass ratio, Λ/M, is equivalent to one plus the proportional force gain:

$$\Lambda/M = 1 + K_{fp}. \tag{29}$$

Using the values of K_{fp} from the explicit force control experiments, corresponding values of Λ/M were chosen to allow direct comparison of the measured response of the impedance and force control schemes.

Figure 9 shows the response of this impedance controller, as well as the commanded position trajectory multiplied by the active stiffness in the same direction. As is readily apparent, the response of this controller is essentially equivalent to that of the proportional gain controller shown in Figure 8. This confirms the previous theoretical assertion.

5.2.2. Impedance Control With Dynamics Compensation

Second-order impedance control can also be implemented with dynamics compensation as shown in equation (17). In this case, equation (18) shows that the mass ratio ΛM^{-1} can be thought of as a proportional force gain. However, it is seen from equations (12)–(14) that only M is selectable in this scheme, since Λ is dependent on the arm mass and configuration.

Usually M is chosen to be diagonal in the task frame along with K and C. When operating in free space ($\mathbf{f}_m = 0$) a diagonal M acts as a simple scaling factor for K and C, thereby preventing coupled motion. If M were nondiagonal, its product with diagonal K and C would be nondiagonal, and coupled motion would result. Furthermore, K and C are usually chosen to be diagonal in some task frame that is aligned with the environment to be contacted. In this way, the manipulator may be made stiff tangential to a surface, but soft normal to it. The velocity gains are usually chosen for critical damping.

However, when in contact with the environment ($\mathbf{f}_m \neq 0$), the ratio of the inertias, ΛM^{-1}, acts as a proportional force gain that is not diagonal in general, because Λ is not generally diagonal in the task frame. Therefore, it is necessary to determine the effective value of the mass ratio (force gain). This requires finding the dominant element of Λ for the direction in which the environment is contacted.

Finding the dominant component of the inertia matrix is equivalent to finding the effective mass in the direction of concern. Since it is the force that is being controlled, this can be done only by determining the resultant acceleration from an applied force:
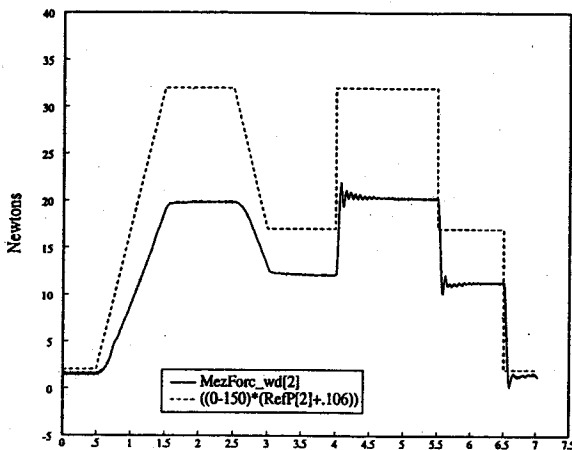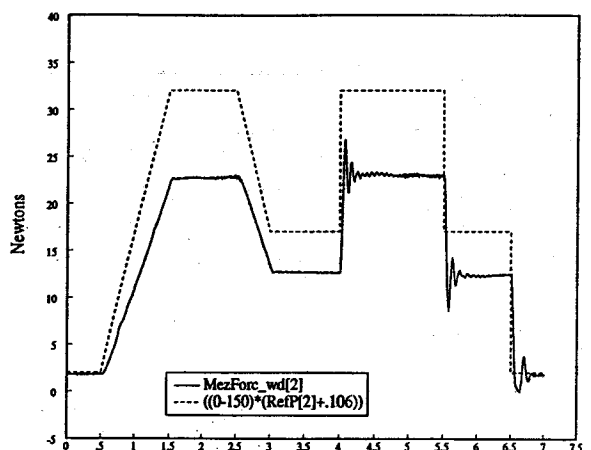
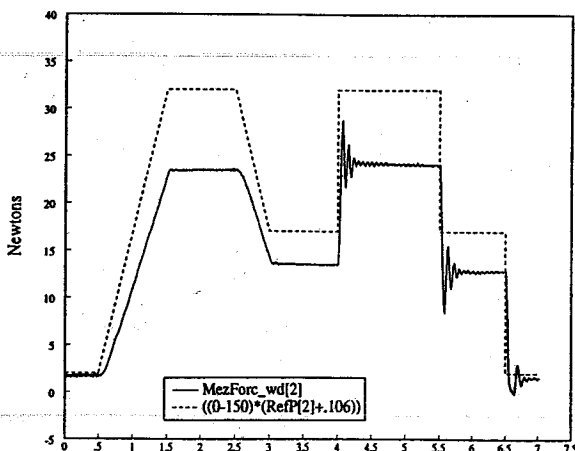$$\ddot{\mathbf{x}} = \Lambda^{-1}\mathbf{f} \tag{30}$$
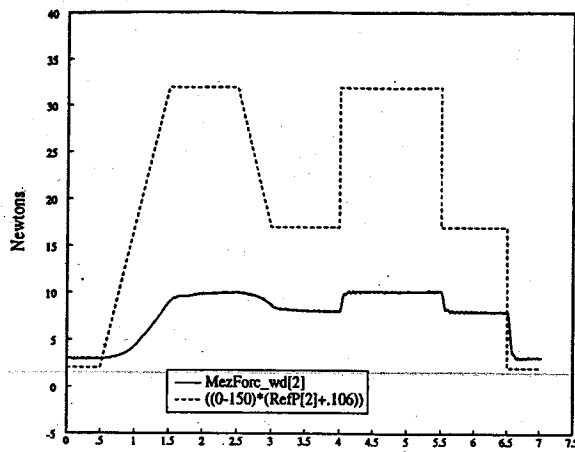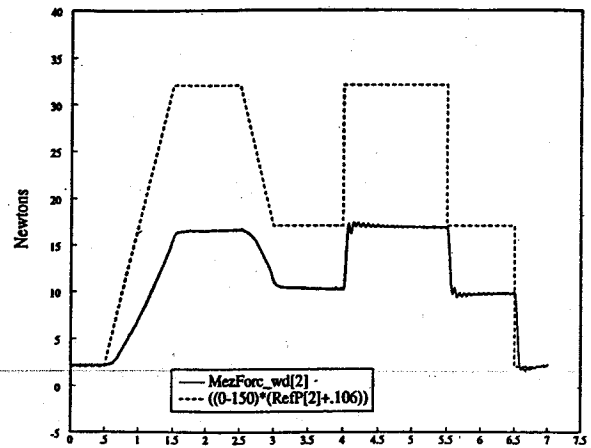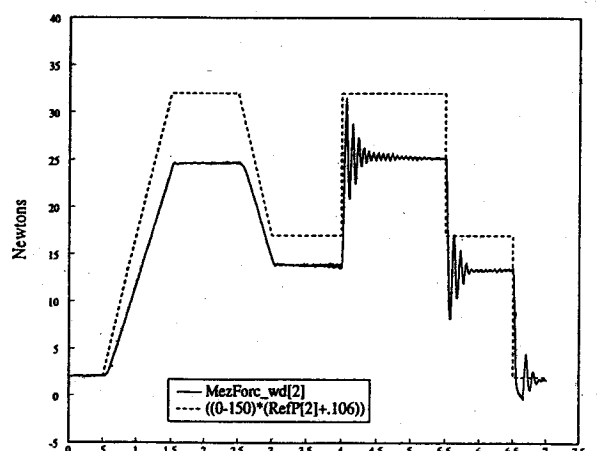
Fig. 9. Experimental data of impedance control without dynamics compensation. The mass ratio "gain" varies from 0.25 to 2.0.

(g) $\Lambda/M = 1.75$ Time(seconds)

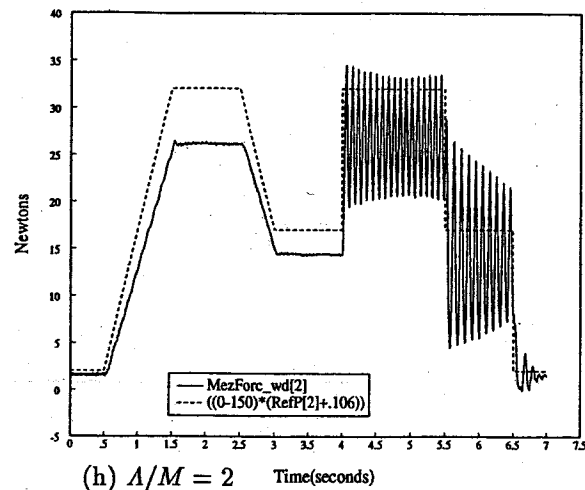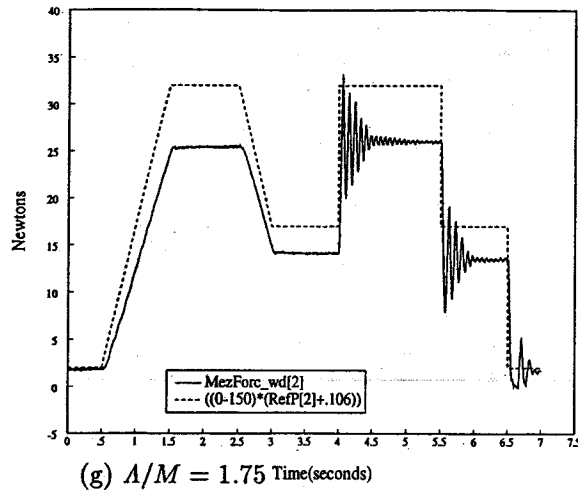

(h) $\Lambda/M = 2$ Time(seconds)

Fig. 9. continued. Experimental data of impedance control without dynamics compensation. The mass ratio "gain" varies from 0.25 to 2.0.

The force may be set to be the unit vector in the direction of the surface, which was the z direction in the experiments performed. The actual values of equation (30) were:

$$\ddot{\mathbf{x}} = \begin{bmatrix} 0.070 & 0 & -0.053 & 0 & 0 & 0 \\ 0 & 1.671 & 0 & -9.723 & -0.049 & 0 \\ -0.053 & 0 & 0.199 & 0 & 0 & 0 \\ 0 & -9.723 & 0 & 59.9 & -1.272 & 0 \\ 0 & -0.049 & 0 & -1.272 & 2.758 & 0 \\ 0 & 0 & 0 & 0 & 0 & 3226 \end{bmatrix} \begin{bmatrix} 0 \\ 0 \\ 1 \\ 0 \\ 0 \\ 0 \end{bmatrix}.$$

(31)

It is apparent that for z direction forces applied to the arm in this configuration, the dominant acceleration is $\ddot{x}_z \approx 0.2\,\mathrm{m/s^2}$. Thus, the apparent inverse scalar mass is $\Lambda_{33}^{-1} \approx 0.2\,\mathrm{kg^{-1}}$. This implies that the best scalar approximation of the mass in the z direction is $\Lambda_z = \Lambda_{33} \approx 5\,\mathrm{kg}$. This value may then be thought of as a scaling factor applied to the variable gain value $M_z = M_{33}$ in equation (17).
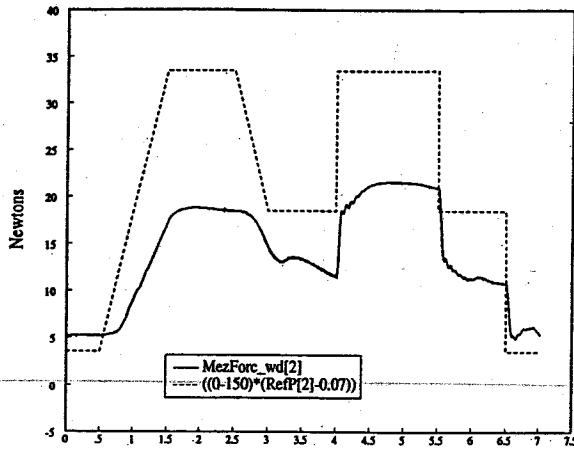
Figure 10 shows the response of impedance control with dynamics compensation for $0.1 \le 1/M_z \le 0.45$, or equivalently, $0.5 \le \Lambda/M \le 2.25$ and $-0.5 \le K_{fp} \le 1.25$. (As with the previous tests, $K = 150\,\mathrm{N/m}$ and $C = 10\mathrm{N/m\cdot s}$.) Thus, a direct comparison can be made between the system response shown in Figure 10A–G and that shown in Figures 8 and 9B–H. The responses are very similar, supporting the previous analytical assertions.

5.3. Impact Control

In the experimental data presented thus far, the lowest gain values have exhibited the greatest stability. For pro-

portional gain explicit force control, this means negative gain values. For impedance control, this means mass ratios < 1. A comparison of the root loci in Figures 4 and 7 shows that the low gain values place the complex poles further left and closer to the real axis, reflecting this greater stability. It has also been shown in the force tracking experiments that the stability gained is offset by a decrease in accuracy. There is one mode of operation of a manipulator that requires maximal stability without a great need for accuracy. This mode is impact control.

We have previously proposed this form of impact control and shown its efficacy at maintaining stability during the transition from motion through the environment to contact with it (Volpe and Khosla 1991; 1993b). Some of those results are reviewed here as further evidence of the equivalence of proportional gain force control and impedance control. Figure 11 shows the response of impacts of the manipulator with the same environment. The solid line is the measured force, and the dotted line is the measured velocity. The dashed line is the reference force in the explicit force control experiment and the reference position multiplied by stiffness for the impedance control experiment. As can be seen, the same correspondence exists for the impact results as existed for the force trajectory following experiments. This further confirms the equivalence of proportional gain force control and impedance control. It also indicates that excellent impact stability can be attained with these controllers, but not with the same gains that work best force tracking. We have shown that the impact period is best treated as a separate case, independent of motion through free space or constrained application of forces (Volpe and Khosla 1993b).
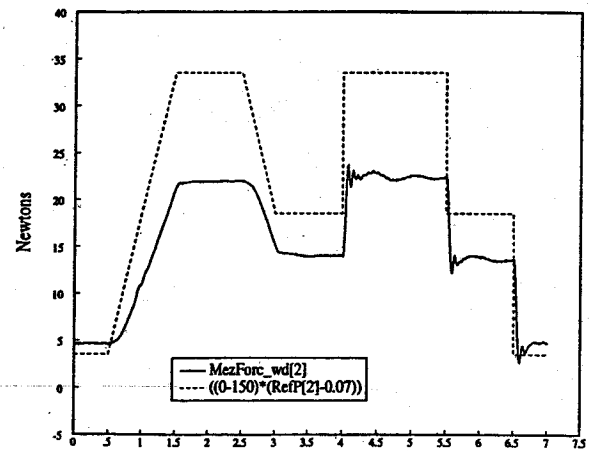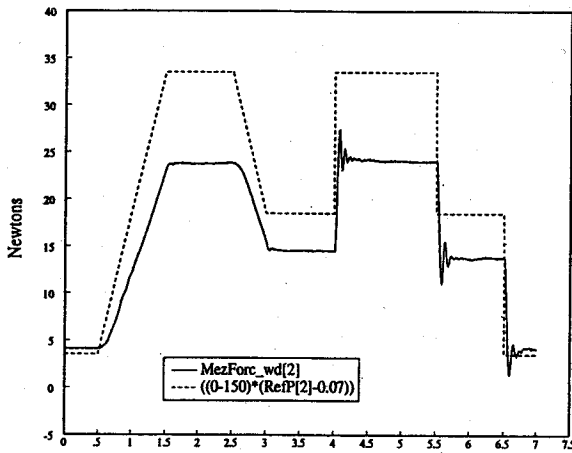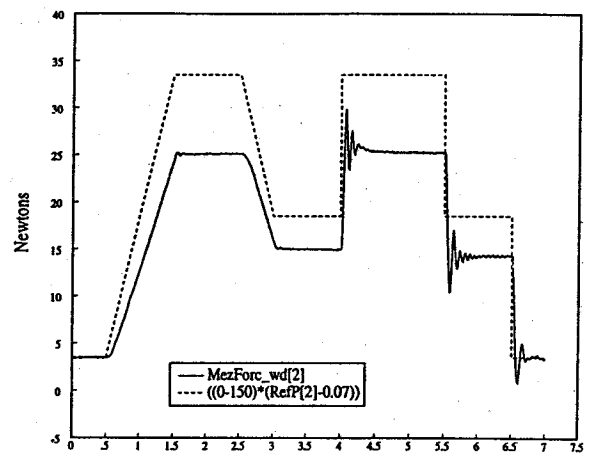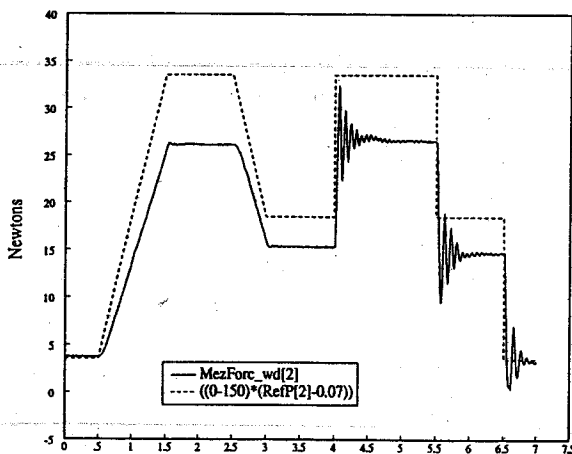
Fig. 10. Experimental data of impedance control with dynamics compensation. The commanded inverse mass varies from 0.1 to 0.45. This is approximately the same as $0.5 \leq \Lambda/M \leq 2.25$ and $-0.5 \leq K_{fp} \leq 1.25$.
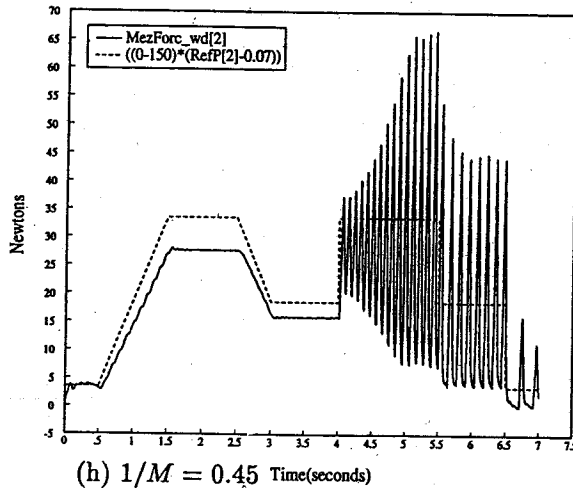
(g) $1/M = 0.4$ Time(seconds)
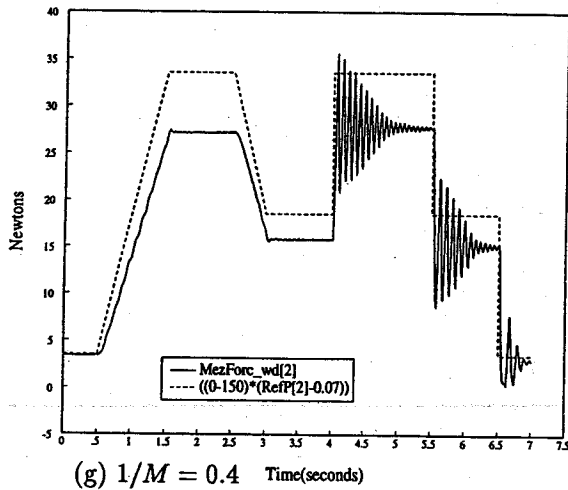

(h) $1/M = 0.45$ Time(seconds)

Fig. 10. continued. Experimental data of impedance control with dynamics compensation. The commanded inverse mass varies from 0.1 to 0.45. This is approximately the same as $0.5 \leq \Lambda/M \leq 2.25$ and $-0.5 \leq K_{fp} \leq 1.25$.

(a) $K_{fp} = -0.75$ Time(seconds)

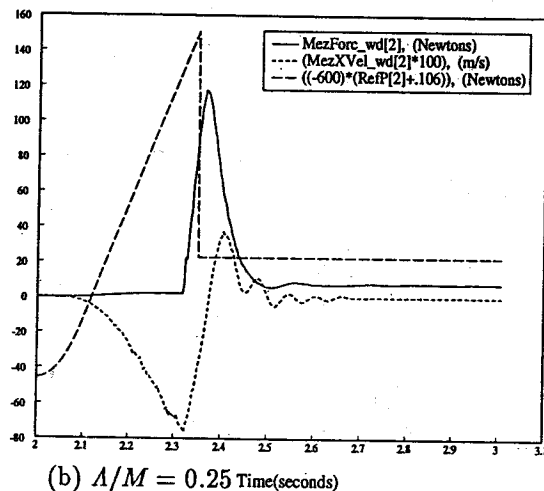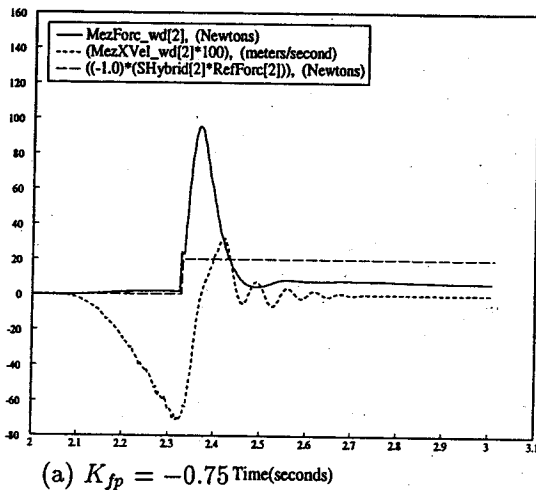(b) $\Lambda/M = 0.25$ Time(seconds)

Fig. 11. Experimental data comparing the best response for impacts controlled by proportional gain explicit force control with feedforward force, and those controlled by impedance control. The controllers have essentially equivalent response and are well suited for ensuring impact stability with the proper selection of control parameters.

6. Conclusions

The results presented in this article demonstrate that second-order impedance control and proportional gain explicit force control with feedforward are essentially equivalent. This leads us to question the value of impedance control as a unified controller for motion through, and constrained interaction with, the environment. Our conclusion that impedance control is not the best solution for these modes of operation is illustrated by the following discussion.

First, it has been shown that proportional gain force control is not the best force controller; integral gain control provides much better tracking (Volpe and Khosla 1993a). Therefore, the behavior of the impedance

controller while in contact with the environment is not optimal and not always stable.

Second, impedance control is more cumbersome to use, since it requires position reference instead of force reference. Some researchers see this as a strength, since there is no need to switch inputs between the modes of free space motion and constrained force application. However, this implies there is knowledge of the position commands necessary for a contact operation that intrinsically requires force commands.

Third, while not in contact with the environment, impedance control continues to incorporate force feedback information into the control law. Phenomena such as sensor noise or inertial loading by the end effector can

cause nonzero force readings and inhibit the performance of the position control (Volpe and Khosla 1994b).

Fourth, impedance control gains that are stable during unconstrained and constrained actuation cause oscillation or instability during the transition phase of impact (Volpe and Khosla 1993a,b). Adaptively modifying the gains may provide a fix but detracts from the notion that impedance control can work in all manipulation situations. Furthermore, if switching is to be employed, it seems attractive to switch controllers as well as gains and get the best performance possible from the system.

Therefore, the results of this work indicate two major points. First, second-order impedance control must be recognized as essentially equivalent to proportional gain explicit force control with force feedforward. Second, if impedance control is to be used, it has inherent limitations that make it something less than the best controller for any given manipulation mode.

Acknowledgments

References

An, C., and Hollerbach, J. 1987. Dynamic stability issues in force control of manipulators. In *Proceedings of the IEEE Conference on Robotics and Automation*, pp. 890–896.

Anderson, R., and Spong, M. 1988. Hybrid impedance control of robotic manipulators. *IEEE J. Robot. Automation* 4(5):549–556.

Bejczy, A. 1974 (February). Robot arm dynamics and control. Technical memorandum 33-669. Jet Propulsion Laboratory, Pasadena, CA.

Dubowsky, S., and DesForges, D. T. 1979. The application of model reference adaptive control to robot manipulators. *ASME J. Dynam. Sys. Measurement Control* 101:193–200.

Eppinger, S., and Seering, W. 1986. On dynamic models of robot force control. In *Proceedings of the IEEE Conference on Robotics and Automation*, pp. 29–34.

Eppinger, S., and Seering, W. 1987. Understanding bandwidth limitations on robot force control. In *Proceedings of the IEEE Conference on Robotics and Automation*, Raleigh, N.C., pp. 904–909.

Goldenberg, A. 1988. Implementation of force and impedance control in robot manipulators. In *Proceedings of the IEEE Conference on Robotics and Automation*, pp. 1626–1632.

Goldenberg, A. 1992 (May). Analysis of force control based on linear models. In *Proceedings of the IEEE International Conference on Robotics and Automation*, Nice, France, pp. 1348–1353.

Hamilton, W. 1988. Globally stable compliant motion control for robotic assembly. In *Proceedings of the IEEE Conference on Robotics and Automation*, pp. 1179–1184.

Hogan, N. 1985. Impedance control: An approach to manipulation: Parts I, II, and III. *J. Dynam. Sys. Measurement Control* 107:1–24.

Hogan, N. 1987. Stable execution of contact tasks using impedance control. In *Proceedings of the IEEE Conference on Robotics and Automation*, pp. 1047–1054.

Hsia, T. C. 1986. Adaptive control of robot manipulators—a review. In Bejczy, A. K. (ed.): *Proceedings 1986 IEEE International Conference on Robotics and Automation*. San Francisco: IEEE, pp. 183–189.

Kazerooni, H., Sheridan, T., and Houpt, P. 1986. Robust compliant motion for manipulators, parts I and II. *IEEE J. Robot. Automation* RA-2(2):83–105.

Khatib, O. 1980 (December). Commande dynamique dans l'espace operationnel des robots manipulateurs en presence d'obstacles. Ph.D. thesis. Ecole Nationale Superieure de l'Aeronautique et del'Espace (ENSAE).

Khatib, O. 1986. Real-time obstacle avoidance for manipulators and mobile robots. *Int. J. Robot. Res.* 5(1):90–98.

Khosla, P. 1988. Effect of sampling rates on the performance of model-based manipulator control schemes. In Schweitzer, G. (ed.): *Dynamics of Controlled Mechanical Systems*. New York: Springer-Verlag, pp. 271–284.

Koivo, A. J., and Guo, T. H. 1981 (June). Control of robotic manipulators with adaptive control. In *Proc. IEEE Conference on Decision and Control*, pp. 271–276.

Luh, J., Walker, M., and Paul, R. 1980. Resolved-acceleration control of mechanical manipulators. *IEEE Trans. Auto. Control* 25(3):468–474.

Mason, M. 1981. Compliance and force control for computer controlled manipulators. *IEEE Trans. Sys. Man Cybernet.* 11(6):418–432.

Slotine, J., and Li, W. 1987 (April). Adaptive strategies in constrained manipulation. In *Proceedings of the IEEE International Conference on Robotics and Automation*, pp. 595–601.

Stewart, D., Volpe, R., and Khosla, P. 1992 (July). Integration of real-time software modules for reconfigurable sensor-based control systems. In *Proceedings of the 1992 IEEE International Conference on Intelligent Robots and Systems*.

Tourassis, V. 1988. Principles and design of model-based robot controllers. *Int. J. Control* 47(5):1267–1275.

Volpe, R. 1990 (September). Real and artificial forces in the control of manipulators: Theory and experiments. PhD thesis. Department of Physics, Carnegie Mellon University, Pittsburgh, PA.

Volpe, R., and Khosla, P. 1990. Manipulator control with superquadric artificial potential Functions: Theory and experiments. *IEEE Trans. Sys. Man Cybernet.* 20(6):1423–1436.

Volpe, R., and Khosla, P. 1991 (June). The equivalence of second order impedance control and proportional gain explicit force control: Theory and experiments. In *Proceedings of the Second Annual International Symposium on Experimental Robotics*, Toulouse, France.

Volpe, R., and Khosla, P. 1993a. A theoretical and experimental investigation of explicit force control strategies for manipulators. *IEEE Trans. Auto. Control* 38(11):1634–1650.

Volpe, R., and Khosla, P. 1993b. A theoretical and experimental investigation of impact control for manipulators. *Int. J. Robot. Res.* 12(4):351–365.

Volpe, R., and Khosla, P. 1994a. Analysis and experimental verification of a fourth order plant model for manipulator force control. *IEEE Robot. Automation Magazine* 1(2):4–13.

Volpe, R., and Khosla, P. 1994b. Computational considerations in the implementation of force control strategies. *J. Intell. Robot. Sys. Theory Applications* 9:121–148.